Supporting Information

1. Classical ions

Classical Simulations. The system simulated consists of a slab of water in contact with a metal surface on each side. The metal surface consists of three layers of atoms, totaling nearly 500 particles, held fixed in a face centered cubic lattice with a Pt spacing of 3.92 Å and the 111 facet exposed to the solution. A slab of water nearly 40 Å thick was placed in contact with the metal, and the dynamics of the nearly 1800 molecules were propagated using a langevin thermostat, with SETTLE[1] imposing bond and angle constraints for the water as implemented in LAMMPS [2]. All simulations were run at 298 K. Interactions between the water molecules are computed from the SPC/E potential [3]. The water-metal potential is modeled following Siepmann and Sprik [4] where the platinum water interaction is a sum of two and three body terms, parameterized to get the correct value of the adsorption energy and ground state geometry as determined by quantum chemical calculations. Additionally, to model the polarizable metal surface each atom carries a Gaussian charge of fixed width but variable amplitude, which is updated at each timestep by minimizing the energy of the slab subject to a constraint of equal potential across the conductor. Periodic boundary conditions are employed in the plane parallel to the surface. Ewald summations appropriate for mixed point and Gaussian charge densities were employed[5]. A more thorough description of this model can be found elsewhere [4, 6]. The Na^+ and I^- ions were modeled with point charges and Lennard Jones potentials[7]. A reduced charge was used on the I^- of -0.75 so that the ion pair has a favorable free energy of adsorption to the interface[8].

Free energy calculations. In order to compute the free energy as a function of interionic separation, R, we have preformed umbrella sampling in R and z, the mass weighted distance away from the electrode of the ionic pair. Specifically, we apply a bias potential of the form

$$\Delta U(R,z) = k((z(t)-z^*)^2 + (R(t)-R^*)^2)/2$$

where k is a spring constant equal to 13.5 $k_{\mathrm{B}}T/\text{Å}^2$ and z^* and R^* are umbrella[9] minimum, chosen on a uniform grid of 100 point between $z = \{8:15\}$Å, and $R = \{2, 10\}$Å. Each trajectory was integrated for 2 ns following 50 ps of equilibration. Unbiasing and reweighting were accomplished with the multistate Bennet acceptance ratio[10]. In this way the joint free energy, $F(R,z)$, was computed from

$$\beta\Delta F(R,z) = -\ln P(R,z)$$

which is shown in SI 1. Shown in Fig. 1C of the main text are conditional distributions, or free energies, at select values of $z = 9$, and 15, or $F(R|z)$ with z fixed.

Because the madelung potential, ψ and the interionic distance, R, are highly correlated thermodynamically, we have used the indirect umbrella sampling method[11] to compute the joint free energy $F(R,z,\psi)$ from umbrella sampling simulations used to construct $F(R,z)$. This is constructed by

$$\beta\Delta F(R,z,\psi) = -\ln P(R,z,\psi)$$

without additional sampling. To compute $F(\psi,R)$ we then compute the marginal distribution as

$$F(\psi,R) = -kT\ln\int dz e^{-\beta F(R,z,\psi)}$$

which is shown in Fig. 2 of the main text. Alternatively we can construct the free energy for changing ψ at fixed z, by marginalizing over R as,

$$F(\psi|z') = -kT\ln\int dR e^{-\beta F(R,z=z',\psi)}$$

which is plotted in Fig. 2B of the main text.

Transition path sampling. To analyze the kinetics of ion pair dissociation, we have used transition path sampling[12]. Specifically, we have studied ensembles of trajectories conditioned on starting with inter-ionic distances, $R < 3.5$ Å, and ending with $R > 4.5$ Å over a trajectory 10 ps in length. The starting and ending conditions were chosen to adequately delineate configurations committed to the bound and free states, and the trajectory length was chosen in order to ensure that ions had sufficient time to cross the barrier. Standard shooting and shifting moves were used with a ratio of 1:3. Shooting moves were attempted uniformly along the trajectory and shifting moves were attempted uniformly along the first and last 1/3. Because the trajectories were generated from stochastic dynamics, shooting moves were accomplished by simply reintegrating the trajectories with different randomly drawn noises[13]. This procedure resulted in trajectories decorrelating within around 3 moves, as measured by trajectory autocorrelation functions of the average R and z. In total, 1000 independent trajectories were generated.

To generate members of the transition state ensemble, TSE, we used trajectories of length 10 ps and average over 10 separate realizations of velocities taken from the Maxwell-Boltzmann distribution so as to compute a commitment probability, p_B for a configuration dissociating. If this estimate of p_B falls within a 90% confidence interval of 0.5, we say it is is a member of the TSE. Members of the TSE are projected into the R,ψ plane in Fig. 2A. In order to evaluate ψ as a relevant dynamical coordinate, we have computed the distribution of commitment probabilities constrained to the saddle point in ψ, which is at $\beta\psi = 15$, and compared that distribution to that constrained to $R = 4$. Each estimate of the commitment probability was

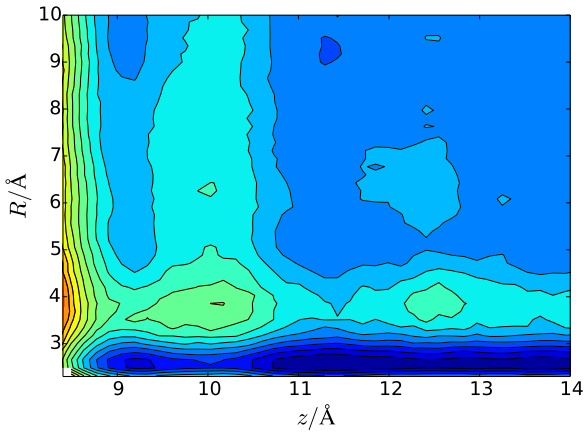

Fig. 1. Joint free energy for moving the ion center of mass towards or away from the electrode, z, and separating the ion pair, R.

computed from 10 independent trajectories, and around 500 configurations were generated for each coordinate from constrained equilibrium sampling. Figure 2 shows the results of these calculations, with the distribution constrained to $\beta\psi = 15$ yielding a peaked distribution around $p_B = 0.5$ and the distribution constrained to $R = 4$ yielding a bimodal distribution around $p_B = 0.0$ and $p_B = 1$. This is strong evidence for ψ being the relevant dynamical variable for charge separation[14].

Rate constants were evaluated by computing the side-side correlation function[15]. Specifically the correlation function,

$$C(t) = \frac{\langle h_a(0) h_b(t) \rangle}{\langle h_a(0) \rangle}$$

where,

$$h_a(t) = \begin{cases} 1 \text{ if } R(t) < 3.5\,\text{Å} \\ 0 \text{ else} \end{cases}$$

and

$$h_b(t) = \begin{cases} 1 \text{ if } R(t) > 4.5\,\text{Å} \\ 0 \text{ else} \end{cases}$$

are the basin definitions used in the transition path sampling calculations. The long time slope of this function is the rate of dissociation, which was computed for 1000 independent trajectories initiated from constrained equilibrium sampling both near or away from the interface. These functions were reported in figure Fig. 2C of the main text.

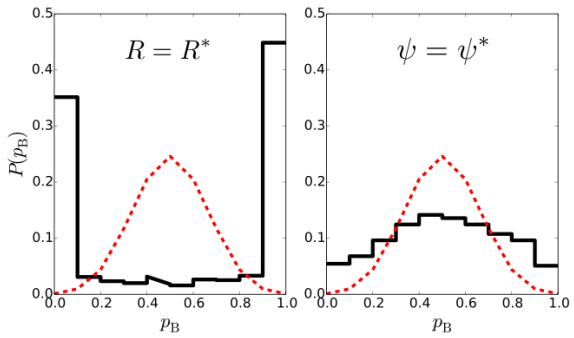

Fig. 2. Conditional commitment probability p_B, evaluated with TPS (black), for $R = R^* = 4$Å (left) and $\beta\psi = \beta\psi^* = 15$ (right) compared to a Bernoulli distribution with 10 trials (red).

2. Water ions

DFTMD simulations. To simulate water ion recombination Density Functional Theory based Molecular Dynamics (DFTMD) simulations were performed. The Gaussian Plane Wave (GPW) implementation [16] in CP2K [17] was used with a DZVP Gaussian basis set [18] and a plane wave cut off at 280 Ry for the bulk simulations and 300 Ry for the interface simulations. The

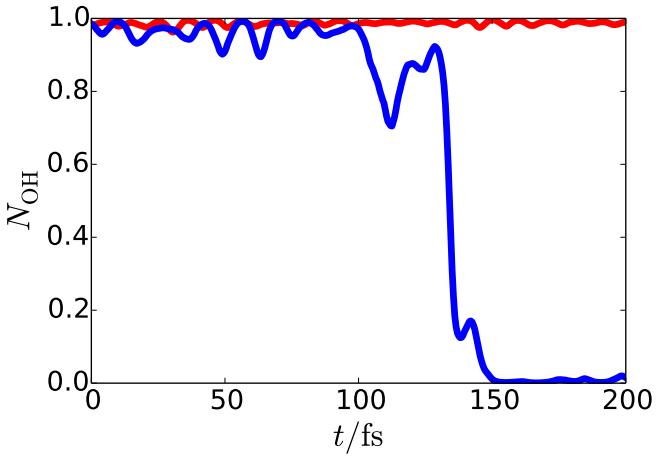

Fig. 3. The quantity n_{OH} decays smoothly from 1 to 0 as an O-H bond breaks (blue) whilst remaining approximately 1 for an intact water molecule (red).

core electrons are described with GTH pseudopotentials [19, 20]. The calculations were done at the PBE level [21]. Grimme's D3 dispersion corrections [22] were used for the interface calculations. This correction has been found to improve simulated values of water density at a liquid-vapor interface[23] while having little effect on bulk structure and dynamics relative to pure PBE[24]. Since our Platinum-water simulation feature a narrow slab of water and thus also includes a liquid-vapor interface we included this correction to limit artifacts arising due to the presence of the liquid-vapor interface. The fixed metal surface was modeled with the same lattice constant of 3.92 Å, with the 111 facet exposed to water as described above. The IC-QM/MM method [25] was used to model Siepman-Sprik metal and the same empirical potential was used for the adsorption of water molecules as for the monovalent ions [4]. The ensemble was simulated using a time step of 0.5 fs with a target temperature of 330 K, which was controlled using the canonical sampling velocity rescaling thermostat [26].

The bulk systems consisted of 32 and 64 water molecules inside cubes of length 9.85 Å and 12.41 Å respectively. An orthorhombic supercell was constructed for the interface system by taking a subset of atoms from a larger equilibrated classical constant potential simulation by only including atoms in a box $13.90 \times 14.44 \times 22.0$ Å and then adding a 20 Å vacuum buffer. The number of water molecules in the system were: 106, 98 and 96. Periodic boundary conditions were applied in all three dimensions.

Initial conditions were taken from equilibrated classical molecular dynamics simulations of the form described above, followed by 10 ps of DFTMD equilibration. A proton was then removed from a water molecule and attached to another water molecule a distance R away in order to create a pair of charged water ions. Constraints to impose a fixed proton coordination number were then applied and the system was equilibrated for 10 ps. Initial configurations for recombination trajectories were taken every 100 fs, after the initial 6 ps. The recombination trajectories were run with no constraints and were terminated upon recombination to neutral water molecules. This initialization procedure was redone independently three additional times in the bulk and twice at the interface.

Identifying water ions. To identify the H_3O^+ and OH^- species in the DFTMD simulation the coordination of the hydrogen atom with an oxygen atom is calculated as:

$$n_{\mathrm{OH}}(r) = (1-(r/r_0)^{16})/(1-(r/r_0)^{56})$$

from reference [27], where r is the distance between the H atom and the O atom and $r_0 = 1.32$Å. Calculating n_{OH} for every oxygen atom with each hydrogen atom and taking the maximum value allows for the assignment of each hydrogen atom with one oxygen atom. The oxygen atom that coordinates with three hydrogen atoms is the H_3O^+ center and the oxygen atom that only coordinates with one hydrogen atom is the OH^-. In some instances the distances can be very delocalised and more than one H_3O^+ and OH^- centers are identified. In these cases a cluster of ions can be identified *i.e.*, a hydronium with the structure $[H_3O-OH-H_3O]^+$ or a hydroxide with the structure $[OH-H_3O-OH]^-$. In these cases we define the water ion as the central oxygen and the three or one nearest hydrogens for hydronium or hydroxide respectively.

An example of how the quantity n_{OH} decays from 1 to 0 as the O-H bond breaks is shown in figure 3. This is compared with a an O-H bond that vibrates whilst remaining in tact.

Recombination time from DFTMD simulations. The number of ions in the simulation is obtained using the same order parameter as in reference [27] where the number of ions:

$$N_{\mathrm{ions}} = \sum_{\mathrm{i}=1}^{N_{\mathrm{O}}} (n_i - 2)^2,$$

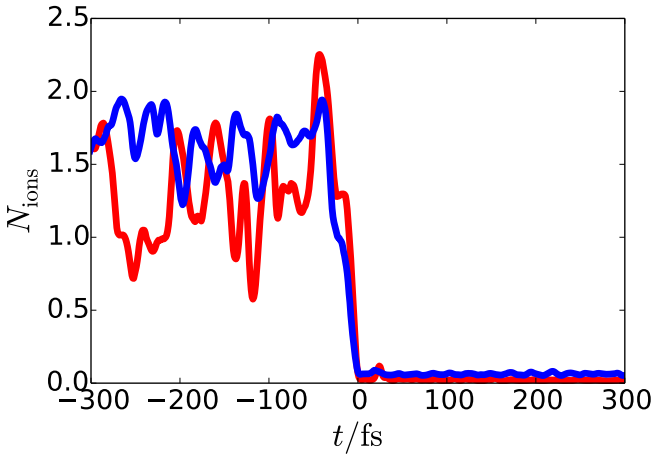

Fig. 4. The recombination of water ions is followed by analyzing the number of ions in the simulation as seen for a typical trajectory. The recombination time is shifted to $t = 0$.

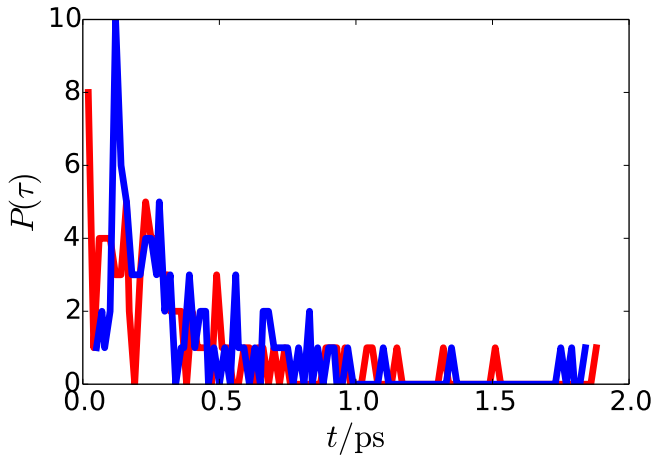

Fig. 5. The probability of recombination time τ for the bulk (red) and the electrode (blue) for 200 simulations with ion-ion initial distances at 5 Å.

where N_O is the total number of oxygen atoms in the system and n_i indicates the number of hydrogens coordinated to the ith oxygen,

$$n_i(r) = \sum_{j=1}^{N_{\mathrm{H}}} (1 - (r_{ij}/r_0)^{16})/(1 - (r_{ij}/r_0)^{56}),$$

where the summation is taken over all N_{H} hydrogens in the system, r_{ij} is the distance between oxygen i and hydrogen j. The recombination time for a given simulation is obtained as the first instance in time where N_{ions} approximately equals 0. An example of this shown in figure 4.

Figure 5 shows the DFTMD data for recombination times of 200 simulations where the initial ion-ion distances were fixed at 5 Å. The noisiness of this data motivates the use of the KMC model.

Hydrogen bond lifetime. The hydrogen bond network is analyzed using a standard definition where the O-O length must be less than 3.5Å and the O-H-O angle must be less than 30°.The hydrogen bond lifetime τ_{HB} is obtained by identifying the hydrogen bonds at $t = 0$, using this hydrogen bond definitions, and finding the time that the hydrogen bond breaks.

Distortion of the interfacial hydrogen bonding network. At an interface the three-dimensional hydrogen bonding network must terminate along a two-dimensional plane. This leads to distortions in hydrogen bonding structure that affect the recombination of hydroxide and hydronium. In particular, the distortion reduces the number of available hydrogen bond chains through which concerted recombination can occur. To quantify this effect we first define a hydrogen bond chain as a series of three consecutive hydrogen bonds (following definition above) formed between four unique water molecules. For any water molecule in the system we define $n_i^{(\mathrm{chain})}$ as the number of such chains for which molecule i resides at the terminal position. We then

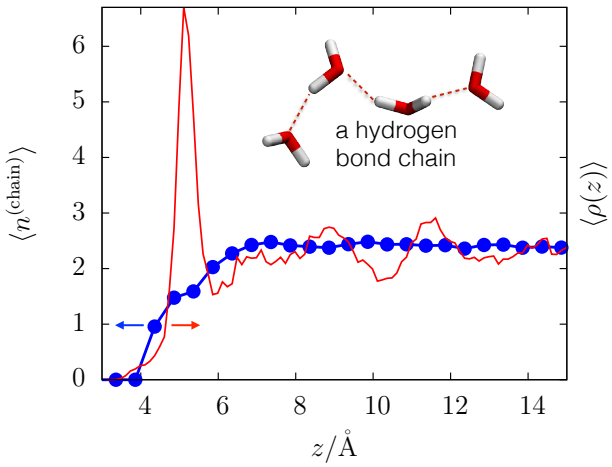

Fig. 6. Blue points indicate the average number of hydrogen bond chains (an example of a hydrogen bond chain is shown inset) whose ends include water molecules at a specific value of z relative to the surface of an electrode. The red line is an overlay of the water density profile in this region. The adsorbed water monolayer resides outside of this scale at a value of $z \approx 2.5$Å.

compute $\langle n^{(\mathrm{chain})}(z) \rangle$, which is the average value of $n_i^{(\mathrm{chain})}$ for water molecules at a specific vertical position, z, relative to the surface of the interface. The results of this computation, as plotted in Fig. 6, reveal a decrease in hydrogen bond chains for water molecules in the vicinity of the electrode interface. Although these results pertain to pure liquid water, due to the water-like solvation structure of hydroxide and hydronium, we expect an analogous decrease in for water-ion pairs.

Free energy calculations. To compute the free energy profile from a Markov state model the water ions are identified, as outlined above, and the inter-ionic distance R is calculated based on the oxygen centers. Markov states are defined by discretizing R in bins 0.2 Å width and their transition probabilities are constructed from:

$$M_{R,R'} = \frac{\sum_k N^k_{R,R'}(\Delta t)}{\sum_k n^k_R}$$

where $N^k_{R,R'}$ is the number of transitions between states R and R' over a lag time Δt from the kth trajectory, and n^k_R is the total amount of time spent in state R in trajectory k. For a fixed discretization of R, the lag time was chosen to be 50fs which ensures that the eigenspectrum of transition matrix shows significant gap, ensuring the transitions are Markovian.

Because the our trajectories are generated without a bias, the transition probabilities obey local detailed balance, $M_{R,R'}/M_{R',R} = p_{R'}/p_R = \exp[-\beta(E(R') - E(R))]$. The transition matrix satisfies an eigenvalue equation of the form,

$$M(R, R')p(R) = \lambda p(R)$$

the λ are the eigenvalues. By conservation of norm, the largest eigenvalue, $\max(\lambda) = 0$, and its eigenvector is the stationary distribution. The free energy profile is given by,

$$F(R) = -k_B T \ln \sum_{R'} M(R, R')p(R').$$

which is plotted in the main text. The accuracy of this estimate of the free energy relies on locally sampling the transition probabilities in proportion to their Boltzmann weights, which requires both forward and backward transitions are well sampled. While the recombination trajectories are able to provide reasonable estimates of $F(R)$ along a large range of R, we are unable to report on the stability of the recombined state as the backwards transition out of the bound state is undersampled.

Kinetic Monte Carlo. We developed a coarse-grained model of water ion recombination that we simulate with a rejection-free kinetic Monte Carlo algorithm[28]. This model was used to obtain the distribution of recombination rates. The model takes static configurations from the DFT trajectories. The identification of the hydronium and hydroxide ions and analysis of the hydrogen bond network were done using the definitions outlined above. A proton can hop to the OH^- or from the H_3O^+ with the structural diffusion rate parameter k. Spontaneous charge recombination can occur through any hydrogen bond chain that connects the H_3O^+ and OH^-. The recombination rate depends on the number of hydrogen bonds in the chain and is given by k'_n for a chain with n hydrogen bonds. Species are also considered recombined if they reside on the same oxygen atom. Values of k and k' were optimized using the maximum likelihood estimation with the DFTMD simulations. Specifically, for a given choice of k and k' we generated the distribution of recombination times, $P(\tau|k, k')_{\mathrm{CG}}$, from the coarse-grained

model. We then quantify the likelihood of observing our specific (and statistically limited) set of *ab-initio* recombination times given that distribution as $L(k,k') = \prod_i^{N_{\rm samp}} P(i|k,k')_{\rm CG}$, where the summation is taken over the set of ab-initio data. Our optimized values of k and k' are those that maximize the functional $L(k,k')$. The optimal values for the bulk were $k = 1/1150$ fs, $k'_{n\leq 3} = 1/325$ fs, and $k'_{n>3} = 0$. The optimal values for the interface were $k = 1/1075$ fs, $k'_{n<=3} = 1/500$ fs, and $k'_{n>3} = 0$. A screened Coulombic attraction has been included in the structural diffusion parameter by using the experimental value of the dielectric constant of water. We generate statistics by performing KMC simulations across an ensemble of starting configuration from our *ab-initio* study.

1. Miyamoto S, Kollman PA (1992) SETTLE: An analytical version of the SHAKE and RATTLE algorithm for rigid water models. *J Comput Chem* 13(8):952–962.
2. Plimpton S (1995) Fast parallel algorithms for short-range molecular dynamics. *J Comput Phys* 117(1):1–19.
3. Berendsen HJC, Grigera JR, Straatsma TP (1987) The missing term in effective pair potentials. *J Phys Chem* 91(24):6269–6271.
4. Siepmann JI, Sprik M (1995) Influence of surface topology and electrostatic potential on water/electrode systems. *J Chem Phys* 102(1):511–524.
5. Gingrich TR, Wilson M (2010) On the ewald summation of gaussian charges for the simulation of metallic surfaces. *Chem. Phys. Lett.* 500(1):178–183.
6. Willard AP, Reed SK, Madden PA, Chandler D (2009) Water at an electrochemical interface-a simulation study. *Faraday Discuss* 141:423–441.
7. Koneshan S, Rasaiah JC, Lynden-Bell RM, Lee SH (1998) Solvent structure, dynamics, and ion mobility in aqueous solutions at 25°C. *J Phys Chem B* 102(21):4193–4204.
8. Otten DE, Shaffer PR, Geissler PL, Saykally RJ (2012) Elucidating the mechanism of selective ion adsorption to the liquid water surface. *Proc Natl Acad Sci USA* 109(3):701–705.
9. Frenkel D, Smit B (2001) *Understanding molecular simulation: from algorithms to applications.* (Academic press) Vol. 1.
10. Shirts MR, Chodera JD (2008) Statistically optimal analysis of samples from multiple equilibrium states. *J Chem Phys* 129(12):124105.
11. Patel AJ, Varilly P, Chandler D, Garde S (2011) Quantifying density fluctuations in volumes of all shapes and sizes using indirect umbrella sampling. *J Stat Phys* 145(2):265–275.
12. Bolhuis PG, Chandler D, Dellago C, Geissler PL (2003) Transition path sampling: Throwing ropes over rough mountain passes, in the dark. *Ann Rev Phys Chem* 53(1):291–318.
13. Crooks GE, Chandler D (2001) Efficient transition path sampling for nonequilibrium stochastic dynamics. *Phys Rev E* 64(2):026109.
14. Geissler PL, Dellago C, Chandler D, Hutter J, Parrinello M (2001) Autoionization in liquid water. *Science* 291(5511):2121–2124.
15. Chandler D (1978) Statistical mechanics of isomerization dynamics in liquids and the transition state approximation. *J Chem Phys* 68(6):2959–2970.
16. Lippert G, Hutter J, Parrinello M (1997) A hybrid gaussian and plane wave density functional scheme. *Mol Phys* 92(3):477–488.
17. VandeVondele J et al. (2005) Quickstep: Fast and accurate density functional calculations using a mixed gaussian and plane waves approach. *Comput Phys Commun* 167(2):103–128.
18. VandeVondele J, Hutter J (2007) Gaussian basis sets for accurate calculations on molecular systems in gas and condensed phases. *J Chem Phys* 127:114105.
19. Goedecker S, Teter M, Hutter J (1996) Separable dual-space gaussian pseudopotentials. *Phys Rev B* 54(3):1703.
20. Hartwigsen C, Gœdecker S, Hutter J (1998) Relativistic separable dual-space gaussian pseudopotentials from H to Rn. *Phys Rev B* 58(7):3641.
21. Perdew JP, Burke K, Ernzerhof M (1996) Generalized gradient approximation made simple. *Phys Rev Lett* 77:3865–3868.
22. Grimme S, Antony J, Ehrlich S, Krieg H (2010) A consistent and accurate ab initio parametrization of density functional dispersion correction (DFT-D) for the 94 elements H-Pu. *J Chem Phys* 132(15):154104.
23. Nagata Y, Ohto T, Bonn M, Kühne TD (2016) Surface tension of ab initio liquid water at the water-air interface. *The Journal of chemical physics* 144(20):204705.
24. Gillan MJ, Alfè D, Michaelides A (2016) Perspective: How good is dft for water? *The Journal of chemical physics* 144(13):130901.
25. Golze D, Iannuzzi M, Nguyen MT, Passerone D, Hutter J (2013) Simulation of adsorption processes at metallic interfaces : An image charge augmented qm / mm approach. *J Chem Theory Comput* 9:5086–5097.
26. Bussi G, Donadio D, Parrinello M (2007) Canonical sampling through velocity rescaling. *J Chem Phys* 126(1):1–7.
27. Hassanali A, Prakash MK, Eshet H, Parrinello M (2011) On the recombination of hydronium and hydroxide ions in water. *Proc Natl Acad Sci USA* 108:20410–20415.
28. Bortz AB, Kalos MH, Lebowitz JL (1975) A new algorithm for monte carlo simulation of ising spin systems. *Journal of Computational Physics* 17(1):10–18.